Available online at www.sciencedirect.com
ScienceDirect
Acta Materialia 58 (2010) 2045–2055
Acta MATERIALIA
www.elsevier.com/locate/actamat

Effect of Re in γ phase, γ' phase and γ/γ' interface of Ni-based single-crystal superalloys

Tao Zhu [a,*], Chong-yu Wang [a,b,c,*], Yong Gan [a,*]

[a] Central Iron and Steel Research Institute, Beijing 100081, China
[b] Department of Physics, Tsinghua University, Beijing 100084, China
[c] The International Centre for Materials Physics, Chinese Academy of Sciences, Shenyang 110016, China

Received 2 April 2009; received in revised form 16 October 2009; accepted 26 November 2009
Available online 11 January 2010

Abstract

Molecular dynamics (MD) within the framework of the embedded atom method and the first-principles discrete variational method (DVM) are both used to study the effect of Re in the γ phase, the γ' phase and the γ/γ' interface of Ni-based single-crystal superalloys. From the MD relaxation it is found that the γ/γ' interface only has two atomic configurations, i.e. a coherent region and a misfit dislocation region, and the "cage-like" misfit dislocation networks, consist of $\langle 1\,1\,0\rangle\{0\,0\,1\}$ edge dislocations winding over the precipitate phase. The MD results also show that the substitution atom Re stabilizes both the γ phase and the γ' phase, and influences the degree of mismatch between γ and γ'. From the simulation results we find that Re atoms have a tendency to cluster in both the γ phase and the γ' phase. Based on the MD simulation we have chosen six clusters of the γ/γ' interface for the DVM study, in which the interatomic energy, the charge distribution, the partial density of states and the electron density difference are all calculated. It is found that a Re atom occupying either a Ni site in the γ phase or an Al site in the γ' phase can strongly enhance the bonding strength between Re and its nearest neighboring atoms, suggesting that the substitution atom Re will influence dislocation motion along the γ/γ' interface.

Keywords: Molecular dynamics simulations; First-principle electron theory; Dislocation structure; Electronic structure; Nickel alloys

1. Introduction

Ni-based single-crystal superalloys, which have remarkable properties at high temperatures, have been designed for use as turbine blades in aeroengines [1,2]. In order to develop engines of higher efficiency, considerable efforts are being devoted to enhancing the high-temperature capabilities of superalloys. It is well known that these alloys are hardened by ordered γ' precipitates ($L1_2$ structure) which are coherently embedded in a nickel solid solution γ matrix (face-centered cubic (fcc) structure). The γ' cuboids are generally aligned along $\langle 0\,0\,1\rangle$ lattice directions and have a cube–cube relationship with the matrix γ phase. Since the nature and interactions between these two phases to a large extent affect the properties of Ni-based single-crystal superalloys, understanding the microscopic structure of the γ and γ' phases is of the utmost importance in the development of novel alloys with superior mechanical properties.

In order to increase the strength of the initial simple Ni–Cr–Al–Ti alloys, one approach has been to strengthen the matrix by adding other elements that can be taken into substitutional solid solution, and to increase the volume fraction of γ'. In modern single-crystal superalloys, the volume fraction of γ' can reach 70% or even higher [3–7]. Some single-crystal superalloys introduced in the late 1980s contain additions of the heavy element rhenium (Re). The single-crystal superalloys are often classified into

* Corresponding authors. Addresses: Central Iron and Steel Research Institute, Dept. of Functional Materials, Xueyuannan Road 76, Beijing 100081, China (T. Zhu, Y. Gan); Department of Physics, Tsinghua University, Beijing 100084, China (C.Y. Wang). Fax: +86 10 6218 2756 (T. Zhu, Y. Gan), +86 10 6277 2782 (C.Y. Wang).
E-mail addresses: zhutao2003@sohu.com (T. Zhu), cywang@mail.tsinghua.edu.cn (C.Y. Wang), gany@cisri.com.cn (Y. Gan).

1359-6454/$36.00 © 2009 Acta Materialia Inc. Published by Elsevier Ltd. All rights reserved.
doi:10.1016/j.actamat.2009.11.047

first-, second- and third-generation alloys. The second and third generations contain about 3 and 6 wt.% of Re, respectively [8,9]. Re is a very expensive addition but can lead to an improvement in the creep strength. It is argued that some of the enhanced resistance to creep comes from the promotion of rafting by Re, which partitions into the γ phase and makes the lattice misfit more negative [3–7,10]. Atomic resolution experiments have revealed the occurrence of small Re clusters in the matrix, and Re can reduce the overall diffusion rate in Ni-based superalloys. It is reported that ~20% substituted Re atoms can strengthen the γ' phase directly and have a tendency to occupy the Al site [5,6]. Therefore, the additions of the refractory element Re play a significant role in improving the properties of superalloys.

Despite extensive investigations, the physical mechanisms responsible for the property of the Re-containing superalloys have not been clearly elucidated. In the present work, molecular dynamics (MD) simulations within the framework of embedded atom method (EAM) [11–13] and first-principles discrete variational method (DVM) [14–19] calculations based on density functional theory (DFT) [20] are both used to study the effect of Re in the γ phase, the γ' phase and the γ/γ' interface of Ni-based single-crystal superalloys. The purpose of this paper is to report and discuss the results of MD simulations as well as DVM analysis on the single-crystal superalloys in order to clarify the role of Re, on the atomic and electronic scales, in improving the properties of superalloys.

In this paper, although there are a number of other elements, such as Cr, Ta, Ti and Mo, in the γ and γ' phase of Ni-based single-crystal superalloys, pure Ni and Ni_3Al are taken as representative of the γ and γ' phase, which might possess the general physical significance.

2. Methodology and model

MD is a powerful tool in materials research, and it is known that interatomic potentials are the key to atomistic simulations. The EAM potential developed by Daw and Baskes [11] is a semi-empirical method which has been widely and effectively used in the simulation of metals and alloys. The basic equation of the EAM is

$$E_{\mathrm{tot}} = \sum_i F(\rho_i) + \frac{1}{2}\sum_{i,j(i\neq j)} \Phi(r_{ij}), \tag{1}$$

where E_{tot} is the total internal energy, $\Phi(r_{ij})$ is the pair potential, r_{ij} is the separation distance between atoms i and j, $F(\rho_i)$ is the embedding function, and the local electron density ρ_i is determined by a superposition of individual atomic electron densities $f(r_{ij})$

$$\rho_i = \sum_{j(\neq i)} f(r_{ij}). \tag{2}$$

Johnson et al. [12] have developed this method and proposed an analytic embedded atom method (AEAM) model for fcc, body-centered cubic (bcc) and hexagonal close-packed (hcp) monatomic metals. In particular, in order to study the alloying, Johnson [13] proposed alloy models based on the EAM, in which he induced a pair potential function $\Phi^{ab}(r)$ between two different species of atom a and b as follows:

$$\Phi^{ab}(r) = \frac{1}{2}\left[\frac{f^b(r)}{f^a(r)}\Phi^a(r) + \frac{f^a(r)}{f^b(r)}\Phi^b(r)\right], \tag{3}$$

where $\Phi^a(r)$ and $\Phi^b(r)$ are the monatomic potentials which can be given by the monatomic models, and $f^a(r)$ and $f^b(r)$ are the electron density of a- and b-type atoms. The unique feature of this model is that it is unaffected by transformation of the pure element functions.

Based on this AEAM model, Zhang et al. [21–23] provided a modified analytic embedded atom method (MAEAM). The MAEAM potential is parameterized using functions and fitted to the cohesive energy, vacancy formation energy, elastic constants, etc., and has been successfully applied to calculate certain properties (stability of structure, point defects, phonon spectra, and thermal expansion) of bcc, fcc and hcp metals, as well as the formation enthalpies, the dilute-limit heats of solution, and the surface segregation of binary alloys. In particular, the MAEAM model is also suitable for the calculation of properties in ordered intermetallic compounds, such as the physical properties (lattice parameter, elastic constants, cohesive energy, etc.), the formation energy of point defects, and the transport and diffusion properties.

In order to test the validity of the MAEAM, a comparison between the MEAM and the Vienna Ab Initio Simulation Package (VASP) [24] values of the properties of Ni_3Re ($L1_2$ structure) is provided in Table 1. In the computation, the projector augmented wave (PAW) version of the generalized gradient approximation (GGA) [25] is used for the electron exchange and correlation. The cutoff energy of atomic wave functions is set to be 350 eV. The calculations are performed using a regular Monkhorst–Pack mesh ($10 \times 10 \times 10$). Convergence is assumed when the energy difference is less than 10^{-5} eV. From Table 1 it can be seen that the MAEAM results are in good agreement with the VASP results.

Hence, the MAEAM potential is suitable for use in MD simulations for monatomic metals, alloys, as well as intermetallic compounds, and the calculated results are in good agreement with the experimental values and other calculated results [23,26].

In Ni-based superalloys the γ phase forms the matrix in which the γ' precipitates. Since both phases have a cubic lattice with similar lattice parameters, the γ' will precipitate in a cube–cube orientation relationship with the γ matrix. This means that its cell edges are exactly parallel to corresponding

Table 1
Lattice parameters, cohesive energies and elastic constants of $L1_2$ Ni_3Re.

	a (Å)	E_c (eV)	C_{11} (eV nm^{-3})	C_{12} (eV nm^{-3})	C_{44} (eV nm^{-3})
MAEAM	3.75	7.45	345.11	200.32	133.98
VASP	3.70	6.99	337.81	195.58	141.02

edges of the γ phase. Because their lattice parameters are similar, small particles of γ' are coherent with the γ.

Considering that γ' phase is the precipitate phase and using the lattice parameters of γ and γ', a "mosaic" initial model is constructed based on the idea of constructing the γ/γ' interface described in our previous work [27]. In this model, a γ' structural unit $(35 \times 35 \times 35)$ replaced by a γ structural unit $(36 \times 36 \times 36)$ in the center of a $40 \times 40 \times 40$ γ block, which is oriented with the [1 0 0], [0 1 0] and [0 0 1] lattice directions. The volume fraction of this model is about 73% ($\sim(36/40)^3$). In order to eliminate the influence of the open surfaces, the model uses periodic boundary conditions along all three directions, and so is a three-dimensional infinite model (see Fig. 1a). This model matches the experimental findings.

In order to provide a credible atomic structure of Re-doped γ/γ' interface for further first-principles calculations, after the doped Re atoms are randomly substituted for the Ni or Al atoms near the γ/γ' interface, the MD simulation is performed using the MAEAM potential for the system. Then, six square dislocation networks, consisting of $\langle 1\,1\,0\rangle\{0\,0\,1\}$ edge dislocations, are formed on the six corresponding γ/γ' interfaces and wind over the precipitate γ' phase. The network resembles a "cage", as shown in Fig. 1b. It is found that only two regions are possible on the γ/γ' interface: (i) a coherent interface region and (ii) a misfit dislocation region (see Fig. 1c).

To clarify the alloying effect of Re on the electronic structure of the γ/γ' coherent region and misfit dislocation region, six various cluster models with the γ/γ' interface, which are derived from the relaxed "mosaic" model, are chosen for the study of DVM.

The DVM [14–19] is a numerical cluster method based on DFT and the local density approximation (LDA). This method has been successfully used to study the electronic structures of metals, alloys and intermetallic compounds [28–30]. The molecular orbitals are expressed by a linear combination of atomic orbitals (LCAO) [14]; the single site basis set with the frozen core mode is used in the atomic orbitals and the funnel potential is added to induce bound states. The Coulomb potential is calculated based on the self-consistent charge (SCC) approximation [15], and the exchange-correlation potential is of the von Barth and Hedin type [31]. The magnetic interaction energy will make

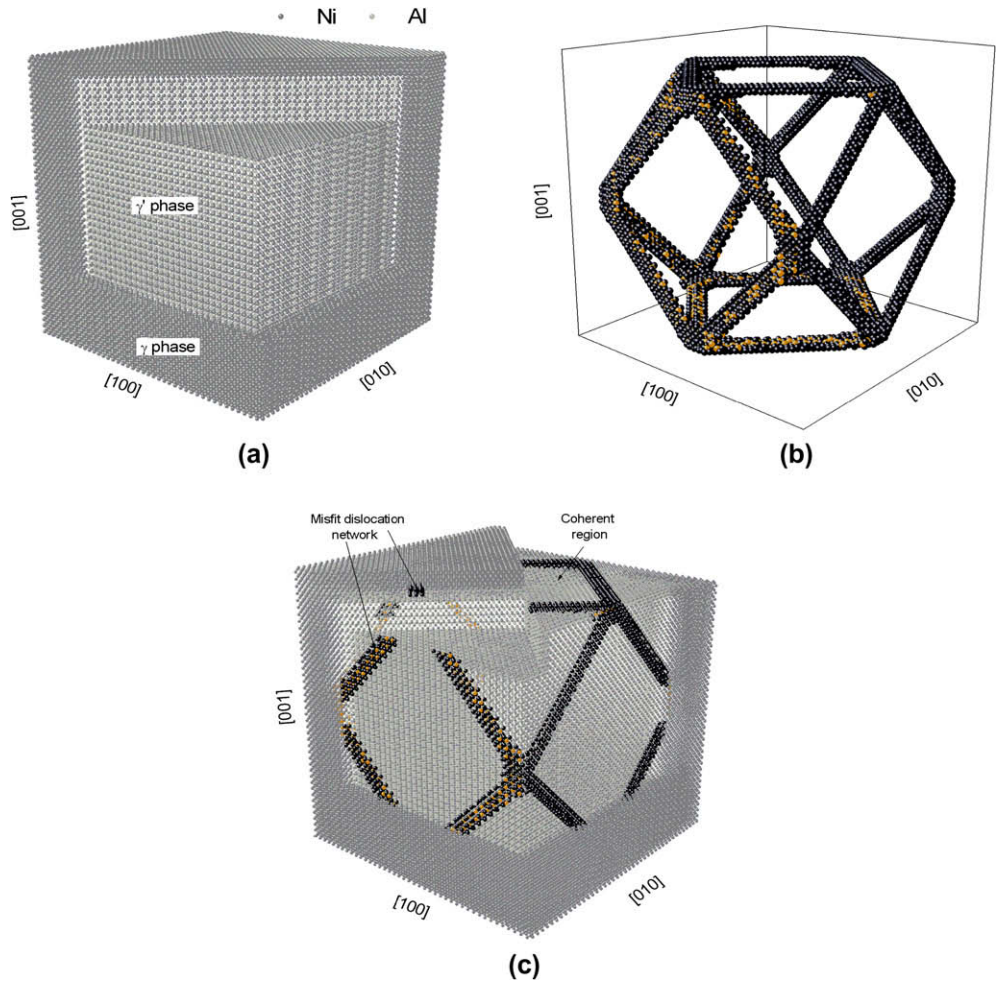

Fig. 1. The formation of the γ/γ' interface of Ni-based single-crystal superalloys: (a) the initial unrelaxed "mosaic" model; (b) the "cage-like" misfit dislocation network after MD relaxation; (c) the relaxed γ/γ' interface with the coherent interface and the "cage-like" misfit dislocation network.

a small contribution to the binding energy [32]. Because the alloy systems are magnetic, all DVM calculations are spin-unrestricted. In the computation, the convergence is accepted if the root mean square of all atomic orbital populations differs by less than 10^{-5} between two successive iterations.

The models are shown in Fig. 2. Model A is the coherent interface model without Re, and models B and C are the coherent interface models with Re substituted for Ni in the γ phase and for Al in the γ' phase, respectively. Model D is the model of the misfit dislocation without Re, and models E and F are the models of the misfit dislocation with Re substituted for Ni in the γ phase and for Al in the γ' phase.

3. Results and discussion

3.1. MD simulation analysis

In order to study the effect of Re in Ni-based single-crystal, it is important to investigate the site occupancy and clustering of Re in the γ phase and the γ' phase.

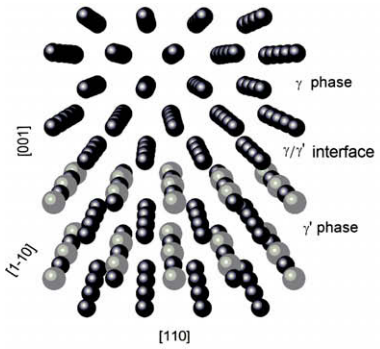

(a) Coherent interface with 154 Ni and 26 Al.

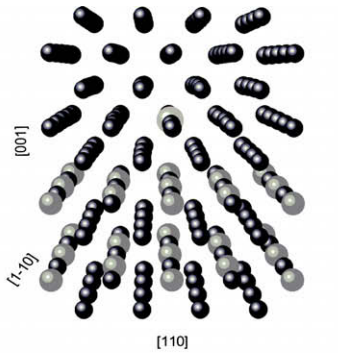

(b) Coherent interface with 153 Ni, 26 Al, and 1 Re.

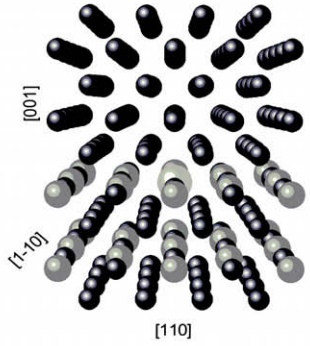

(c) Coherent interface with 154 Ni, 25 Al, and 1 Re.

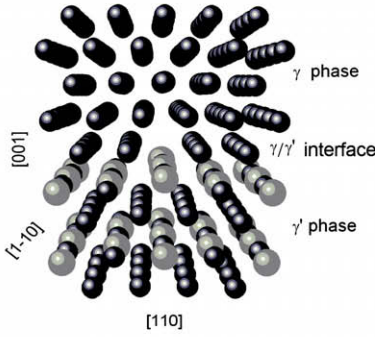

(d) Misfit dislocation with 172 Ni and 26 Al.

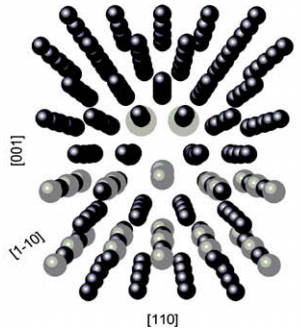

(e) Misfit dislocation with 170 Ni, 26 Al, and 2 Re.

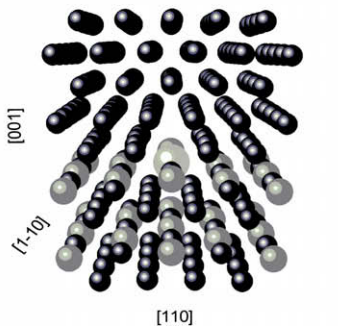

(f) Misfit dislocation with 172 Ni, 25 Al, and 1 Re.

Fig. 2. The interface cluster models used in the DVM calculations. Model A is a clean coherent interface, model B is a coherent interface with Re substituted for Ni in the γ phase, model C is a coherent interface with Re substituted for Al in the γ' phase, model D is a clean misfit dislocation, model E is a misfit dislocation with Re substituted for Ni in the γ phase, model F is a misfit dislocation with Re substituted for Al in the γ' phase. The small, medium and large balls denote a Ni atom, an Al atom and a Re atom, respectively.

In Table 2 we present the total energies obtained by the MD method for the γ phase system ($40 \times 40 \times 40$) and the γ' phase system ($40 \times 40 \times 40$) with the substitution of a Re. It is clear that, in comparison with a pure system, the total energies of Re-doped systems are all lower. In the γ phase, when a Re atom occupies a Ni site, the total energy decreases by 2.38 eV, and in the γ' phase, the total energy decreases by 2.47 and 3.62 eV when a Re occupies a Ni site and an Al site, respectively. Considering the mixing enthalpy, we should subtract the balance between Re and Ni (or Al) from the differences. Thus, the decrease of energy is 1.18 eV when a Re atom occupies a Ni site in the γ phase, and 1.27 eV (or 1.37 eV) when a Re atom occupies a Ni (or Al) site in the γ' phase. These results imply that Re can stabilize both the γ phase and the γ' phase, and has a preference for Al sites in the γ' phase. This is in good agreement with other calculations [30,33]. This is also the reason why it is necessary to ensure that we only have Re substitution for Al in the γ' phase in the DVM calculation.

In addition, we also have analyzed the lattice deformation induced by the Re additions. It is found that when a Re atom replaces a Ni atom in the γ phase, the distance between Re and its 12 nearest neighboring (NN) Ni atoms expands by about 4.09% of the lattice constant. When a Re atom replaces an Al atom in the γ' phase, the distance between Re and the 12 NN Ni atoms expands by about 2.58% of the lattice constant. When a Re replaces a Ni atom in the γ' phase, it can give rise to noticeable lattice distortions. The distance between Re and its eight NN Ni atoms expands by about 3.93% of the lattice constant, while for Re and its four NN Al atoms the distance contracts by about 1.90% of the lattice constant. In all the situations above, we can see that the change of distances between Re atom and its next nearest neighboring (NNN) atoms is less than 1% of the lattice constant, which implies that the alloying of Re into the γ phase or the γ' phase can induce lattice distortion locally. Considering Re in the γ' phase has an Al site preference and the change in lattice constant caused by Re (about 2.58%) is less than that in the γ phase (about 4.09%), it is reasonable to consider that the difference increases the magnitude of lattice mismatch and the corresponding coherence stresses between the γ phase and the γ' phase, which can act as the driving force for precipitate coarsening [34].

Table 2
The total energies (E_t in eV) of the γ phase and the γ' phase with and without the presence of Re atom. ΔE_t denotes the difference in total energies between the Re-doped system and the pure system.

System	Total energy E_t	ΔE_t
Pure γ phase	−1136646.99	
Re is substituted for Ni in the γ phase	−1136649.37	−2.38
Pure γ' phase	−1084765.86	
Re is substitute for Ni in the γ' phase	−1084768.33	−2.47
Re is substitute for Al in the γ' phase	−1084769.48	−3.62

Table 3 presents the total energies of different systems when Re atoms (from 2 up to 225) are dispersed or clustered in the γ phase system ($40 \times 40 \times 40$) and the γ' phase system ($40 \times 40 \times 40$), where N_{Re} is the number of Re atoms and $E_{dispersed}$, $E_{clustered}$ denote the total energy of the system in which Re atoms are dispersed or clustered, respectively. In comparison with the system in which Re atoms are dispersed, it is found that the total energies of Re clustering systems are all lower. For example, when 2 Re, 4 Re, ..., and 225 Re atoms are clustered in the γ phase, the total energy decreases by 0.27, 1.17, ..., and 169.78 eV, respectively, while when these Re atoms are clustered in the γ' phase, the total energy decreases by 0.06, 0.75, ..., and 165.22 eV, respectively. From Table 3, it is also found that the magnitude of the difference ΔE ($= E_{clustered} - E_{dispersed}$) increases with the number of Re atoms N_{Re}. These results imply that clustering of Re atoms can decrease the total energy in both the γ phase and the γ' phase—in other words, Re atoms have a tendency to cluster in both the γ phase and the γ' phase.

In order to study the size property of Re clusters, we have defined the clustering energy E_c as a mean energy decrement

$$E_c = \frac{\Delta E}{N_{Re}} = \frac{E_{clustered} - E_{dispersed}}{N_{Re}}. \quad (4)$$

The curves of E_c vs. Re cluster size in the γ phase and the γ' phase are shown in Fig. 3. Curve (a) shows that with an Re cluster of 12.2 Å, E_c can reach a lower value and then the amplitude of variation changes very gently (the value is about 0.70 eV). In other words, when the size of the Re cluster is larger than 12.2 Å, the total energy will decrease about 0.70 eV as the Re atoms are clustered. This means that the minimum size of the Re cluster in the γ phase is about 12.2 Å. From curve (b), it can also be found that the critical size of the Re cluster in the γ' phase is about 12.2 Å. Since more Ni sites are relatively occupied in the 43 atom cluster, there is a deep minimum around 12 Å. In fact, Re clusters, about 1.0 nm in size, have been detected in Re-modified versions of CMSX-2 and PWA 1480 superalloys [5].

3.2. Electronic structure analysis

The atomic configurations for the electronic structure analysis are taken from the MD relaxation results (see Fig. 2). The interatomic energies (IEs), the charge distribution, the partial density of states (PDOS), the electron density difference, etc., for the above six systems are calculated by the DVM. For clarity, in Fig. 4 we have labelled the atoms in the clusters with arabic numerals.

In order to study the interaction between atoms, the interatomic energy between atom l and m is derived [35,36]:

$$E_{lm} = \sum_n \sum_{\alpha\beta} N_n a^*_{n\alpha l} a_{n\beta m} H_{\beta m\alpha l}, \quad (5)$$

where N_n is the electron occupation number for the molecular orbital ψ_n, $a_{n\alpha l} = \langle \phi_{\alpha l} | \psi_n \rangle$, and $H_{\beta m\alpha l}$ is the Hamiltonian

Table 3
The total energies (in eV) when Re atoms are dispersed and clustered in the γ phase and the γ' phase, where N_{Re} is the number of Re atoms and $E_{dispersed}$, $E_{clustered}$ denote the total energy of the system in which Re atoms are dispersed and clustered, respectively. $\Delta E = E_{clustered} - E_{dispersed}$, and the clustering energy E_c is defined as the mean energy decrement $\Delta E/N_{Re}$.

Phase	N_{Re}	$E_{dispersed}$	$E_{clustered}$	ΔE	$E_c = \Delta E/N_{Re}$
γ phase	2	−1136651.74	−1136652.01	−0.27	−0.14
	4	−1136656.50	−1136657.67	−1.17	−0.29
	13	−1136677.36	−1136684.36	−7	−0.54
	19	−1136691.39	−1136702.27	−10.88	−0.57
	43	−1136747.18	−1136776.04	−28.86	−0.67
	55	−1136777.67	−1136814.14	−36.47	−0.66
	79	−1136834.62	−1136889.2	−54.58	−0.69
	87	−1136853.88	−1136913.69	−59.81	−0.69
	135	−1136967.75	−1137066.64	−98.89	−0.73
	141	−1136981.72	−1137084.78	−103.06	−0.73
	177	−1137066.83	−1137198.28	−131.45	−0.74
	201	−1137125.17	−1137276.46	−151.29	−0.75
	225	−1137182.49	−1137352.27	−169.78	−0.75
γ' phase	2	−1084771.95	−1084772.01	−0.06	−0.03
	4	−1084776.89	−1084777.64	−0.75	−0.19
	13	−1084799.10	−1084805.37	−6.19	−0.48
	19	−1084820.60	−1084830.21	−9.61	−0.51
	43	−1084880.54	−1084914.15	−33.61	−0.78
	55	−1084923.74	−1084961.33	−37.59	−0.68
	79	−1084983.05	−1085028.61	−45.56	−0.58
	87	−1085011.93	−1085061.09	−49.16	−0.57
	135	−1085130.80	−1085219.92	−89.12	−0.66
	141	−1085152.39	−1085246.63	−94.24	−0.67
	177	−1085243.39	−1085379.97	−136.58	−0.77
	201	−1085328.23	−1085475.95	−147.72	−0.73
	225	−1085387.74	−1085552.96	−165.22	−0.73

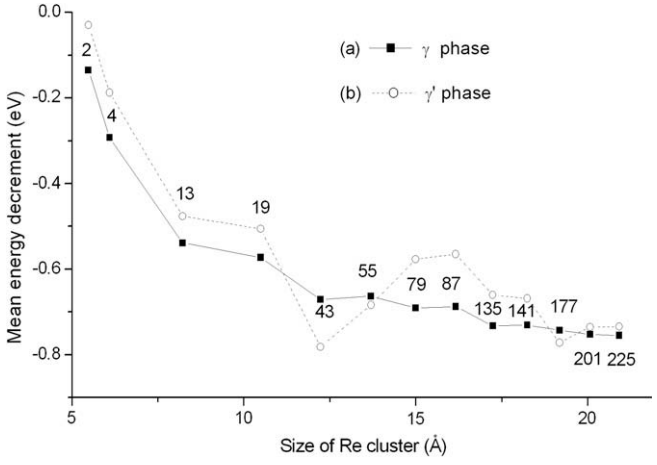

Fig. 3. The variation of mean energy decrement E_c with size of Re cluster in (a) γ phase and (b) γ' phase.

matrix element connecting the atomic orbital $\phi_{\alpha l}$ of atom l to the atomic orbital $\phi_{\beta m}$ of atom m. Since the IE is related to the Hamiltonian matrix element, it can be used to estimate the bonding capability of the two atoms. Usually, a negative number with a large absolute value means a strong interatomic interaction. IE values have proved very useful in studies of Ni_3Al [28–30].

The interatomic energies of some interesting atomic pairs in different γ/γ' interface regions with and without Re atoms are listed in Table 4. In order to show the effect of Re clearly, the changes induced by the substitution by Re for Ni in the γ phase and for Al in the γ' phase are also presented. From Table 4 it can be seen that the interatomic energies of the atoms on the phase boundary are all enhanced when a Ni atom or an Al atom is replaced by a Re, and the interatomic energies of Re and its adjacent atoms are strongly enhanced relative to those of the substituted Ni or Al atoms and the corresponding atoms. As a result, it can be predicted that the strength of the phase boundary in Ni-based single-crystal superalloys will be increased after Re is substituted for Ni or Al atoms. From Table 4 we can also see that the addition of Re might influence slipping along the γ/γ' interface.

It is well known that the charge transfer between the alloying element and the host atom can greatly affect the interatomic bonding behavior. The electron occupation number in valence orbitals is calculated by the use of Mulliken population analysis [37]. The net number of electrons $Q = N - Z_{val}$ (where Z_{val} is the standard number of valence electrons per atom) for each atom is also calculated.

From the results of a coherent system, it can be seen that a Re atom loses more electrons at a Re-doped coherent interface than at a pure coherent interface. With regards to the free Re atoms, when a Re atom is substituted for the Ni3 atom in the γ phase, a proportion of the electrons in the 6*s* orbital are transferred to the 5*d* and 6*p*; however, when a Re atom is substituted for the Al2 atom in the γ'

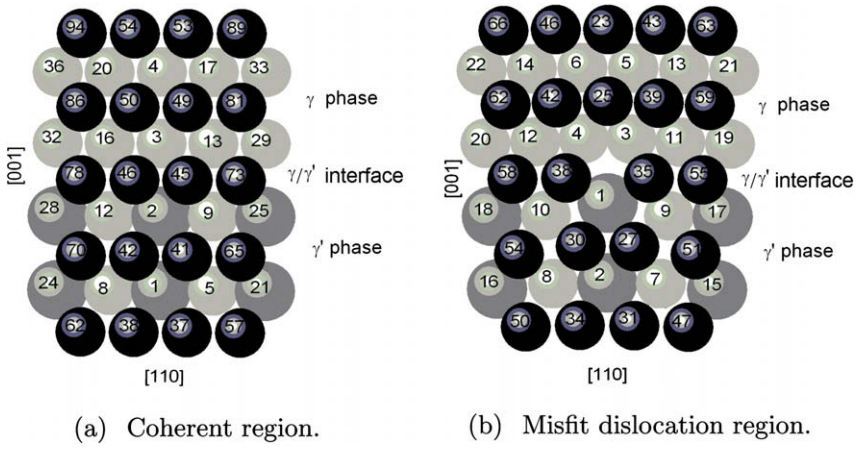

(a) Coherent region. (b) Misfit dislocation region.

Fig. 4. The atomic configurations around the γ/γ' interface. The small and the large spheres denote a Ni site and an Al site, respectively.

Table 4
The interatomic energy (in eV) for selected atomic pairs on the γ/γ' interface with and without Re. $\Delta E_{lm} = E_{lm}$(Re substitution for Ni or Al) $- E_{lm}$(Clean) is the change in interatomic energy induced by Re doping. The Arabic numerals 2–9, 3–13, etc., correspond to the interatomic energies in Fig. 4.

Region	Atom pairs	Clean E_{lm}	Re is substituted for Ni		Re is substituted for Al	
			E_{lm}	ΔE_{lm}	E_{lm}	ΔE_{lm}
Coherent region	2–9	−1.27			−1.97	−0.70
	2–41	−1.19			−1.88	−0.69
	2–45	−1.20			−1.91	−0.71
	3–13	−1.27	−1.82	−0.55		
	3–45	−1.30	−1.84	−0.54		
	3–49	−1.36	−1.95	−0.59		
Misfit dislocation region	1–3	−0.20			−0.69	−0.49
	1–9	−0.25			−0.82	−0.57
	1–27	−1.04			−1.69	−0.65
	1–35	−1.25			−1.96	−0.71
	3–4	−2.11	−3.65	−1.54		
	3–11	−1.59	−2.14	−0.55		
	3–25	−1.34	−1.79	−0.45		
	3–35	−1.79	−2.39	−0.60		
	3–39	−1.37	−1.99	−0.62		

phase, a proportion of the electrons in the 6*s* orbital are transferred to the 5*d* and 6*p*. It can be also found that the total number of valence electrons of NN atoms of the Re atom is increased. The results also show that the electrons lost from Re atom are mainly gained by the *s* orbitals of the neighboring atoms when Re is substituted for Ni in the γ phase, while the electrons lost are shared approximately equally by the *s* and *p* orbitals of the neighboring atoms when Re is substituted for Al in the γ' phase.

From the analysis of charge transfer, we find that, unlike the obvious change of electrons in the *s* or *p* orbitals, the number of electrons in the *d* orbitals is hardly changed. This may represent a reduction in the directionality of the bonds in the Re-doped γ/γ' interface relative to that in the pure γ/γ' interface, because of the dispersed distribution in space of *s* or *p* electrons; in particular, the lost electrons are mainly gained by the *s* orbitals when Re is doped in the γ phase. Furthermore, the total numbers of valence electrons for each host atom which is near to substitution site is increased by additions of Re, which shows that electrons can be shared between atoms such as those found in ductile metals [38].

To complete the analysis of the interactions between atomic orbitals, we have calculated the PDOS by means of the Lorenz broadening scheme combined with a Mulliken population analysis. The PDOS in the DVM is defined as

$$D_{\alpha l}(E) = \sum_n N^n_{\alpha l} \frac{\sigma}{\pi[(E-\varepsilon_n)^2 + \sigma^2]}, \tag{6}$$

where $N^n_{\alpha l}$ is the population of the atomic orbital $\phi_{\alpha l}$ of atom l in energy level ε_n of the molecular orbital, and σ is the broadening parameter.

The PDOS of some particular atoms in the γ phase or in the γ' phase for the coherent interface system and for the dislocation interface system are shown in Figs. 5 and 6, respectively. Fig. 5a shows PDOS curves for the Re3(Ni3), the NN Ni atoms in the pure and in the Re-doped γ phase.

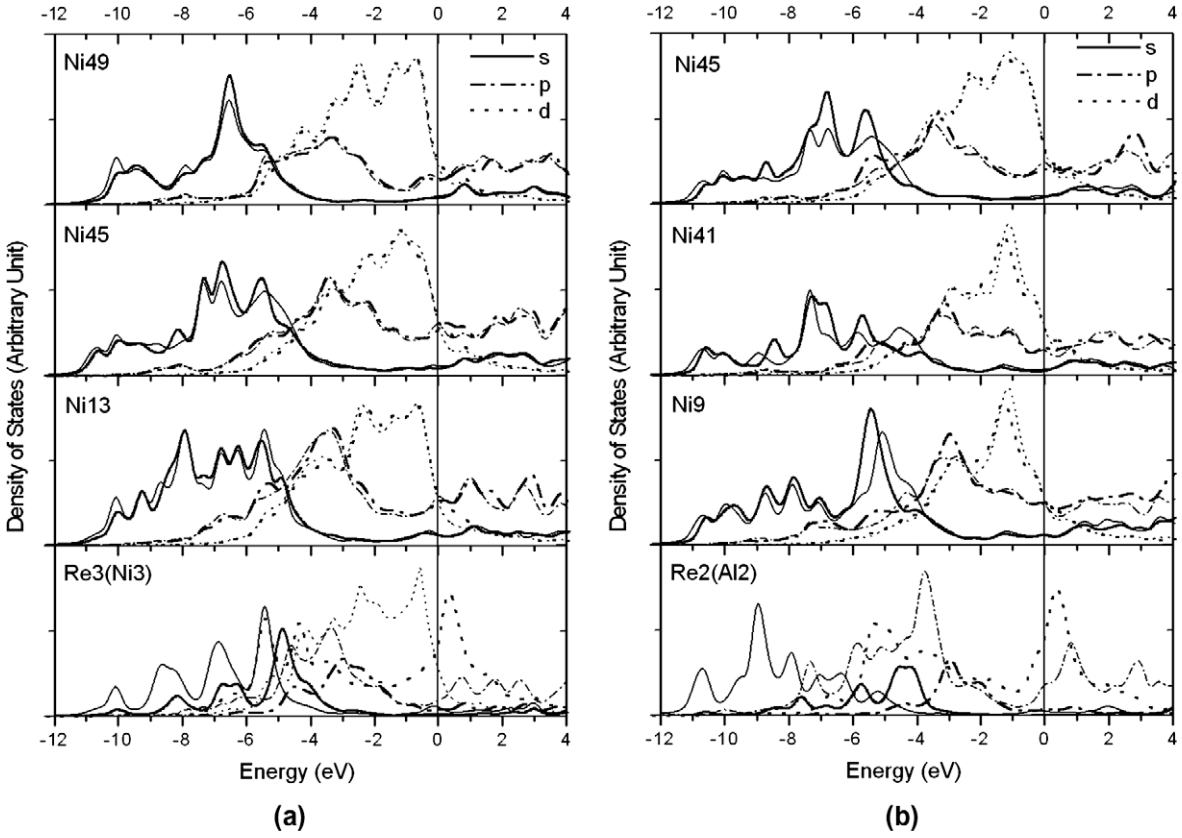

Fig. 5. The partial density of states of some particular atoms in the coherent interface system. (a) Re atom is substituted for Ni3 in the γ phase; (b) Re is substituted for Al2 in the γ' phase. The solid lines, dash-dotted lines and dotted lines denote s, p and d electronic states, respectively. The thick lines and thin lines denote the PDOS with and without Re, respectively. The Fermi level is shifted to zero. The Arabic numerals in Re3, Al2, etc., correspond to those in Fig. 4a.

It is found that the main peaks of s PDOS of the NN atoms (Ni13, Ni45, and Ni49) in the Re-doped system are higher and located in the region of lower energy than those of in the pure system. Considering the dispersed distribution in space of s electrons, this represents a reduction in the directionality of bonds in the Re-doped system relative to that in the pure system. This is in agreement with the results for the analysis of charge distribution. It should be noted that the d electrons of Re bear the predominant responsibility for the bonding between Re and its adjacent atoms. The Re-d hybridize strongly with the s, p, d electrons of its NN atoms, and this makes the interaction between Re and its neighboring atoms very strong, which is consistent with the interatomic energy results. Another feature of the PDOS change is that the magnitude of the d PDOS of Ni at the Fermi level is reduced when Re replaces Ni3 in the γ phase. The reduction of the PDOS near the Fermi level means that the transition probability of the electronic states is confined, and the stability of the γ/γ' interface can be increased [28,29].

Fig. 5b shows the PDOS curves for the Re2(Al2) atom and its NN atoms in the pure and Re-doped γ' phase. Comparing the PDOS of Re-doped system with the pure system, it can be seen that the main peaks of the s and p PDOS of Re are located in the region of higher energy (in which the main peaks of the PDOS of Ni are located too) relative to that of Al2. As a result, the hybridization between Re and its neighboring atoms is stronger than that for Al2 and the corresponding atoms, especially as regards the hybridization between Re p and Ni p partial waves. From Fig. 5 one can also see that the main peaks of the d PDOS of the NN atoms (Ni9, Ni41, and Ni45) turn out to lie lower than their original position, and form a hybrid state among them. This is an indication of strong hybridization among the NN atoms, showing that there is a strong chemical interaction among the NN atoms.

Compared with the coherent system, the PDOS of some corresponding atoms in the γ phase or in the γ' phase for the dislocation system are shown in Fig. 6a and b. It is found that for the NN Ni atoms the d electrons bear the predominant responsibility for the bonding and the main feature of d-PDOS of the corresponding atoms such as Ni49 (in the coherent system) and Ni39 (in the dislocation system), Ni45 (in the coherent system) and Ni35 (in the dislocation system), etc., are similar, except that the main peaks in the coherent system are higher and are located in a region of lower energy than those in the dislocation system, which means the coherent interface is more stable than its corresponding dislocation interface.

The charge density differences of the systems are plotted in Figs. 7 and 8. The charge density difference is defined as

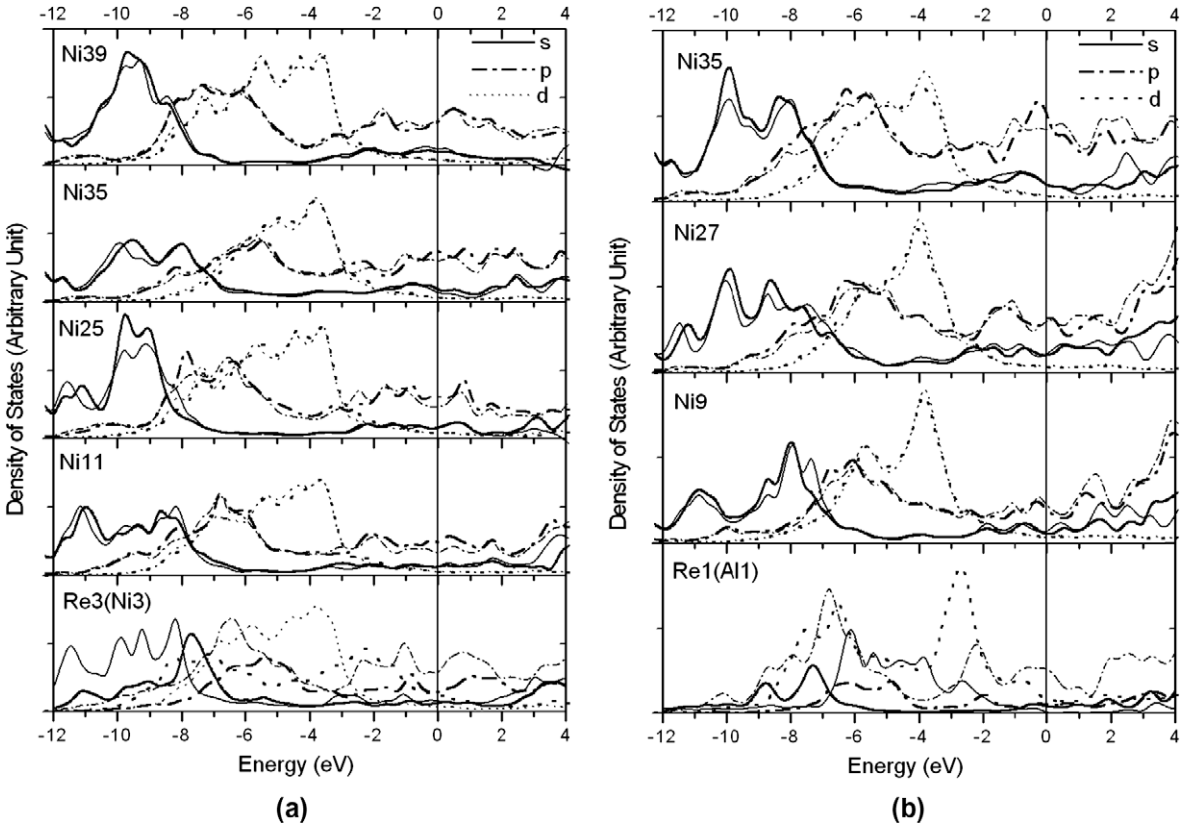

Fig. 6. The atomic partial density of states in the misfit dislocation interface. (a) Re atom is substituted for Ni3, Ni4 in the γ phase; (b) Re is substituted for Al1 in the γ' phase. The solid lines, dash-dotted lines and dotted lines denote s, p and d electronic states, respectively. The thick lines and thin lines denote the PDOS with and without Re, respectively. The Fermi level is shifted to zero. The Arabic numerals in Re3, Al1, etc., correspond to those in Fig. 4b.

$$\Delta\rho = [\rho(\text{Re-doped}) - \rho_{\text{free}}(\text{Re-doped})] - [\rho(\text{clean}) - \rho_{\text{free}}(\text{clean})], \quad (7)$$

where ρ is the charge density of the Re-doped or pure system, and ρ_{free} is the charge density of the free atom.

Fig. 7 shows the electron density difference of the coherent interface system, in which (a) and (b) are for the case where Re is substituted for Ni3 in the γ phase, and (c) and (d) are for the case where of Re is substituted for Al2 in the γ' phase. From Fig. 7a and b, it can be seen that the electron density in the intermediate region between atom Re3 and its NN atoms (Ni13, Ni45, Ni49, etc.) is distinctly increased by the substitution of Re for Ni, so the bonding for Re and its NN atoms is stronger than that for Ni3 and its NN atoms. From Fig. 7b, it can also be found that the electron density between Re3 and Ni45 (as well as Ni45–Ni49, etc.), which are situated on the other side of the γ/γ' interface, is also increased by the substitution of Re for Ni. Therefore, the bonding strength for host atoms which are near to the substitution site is increased by the substitution. In the same way, from Fig. 7c and d, we can see that strong charge accumulations region appear around the Re atoms, reflecting enhanced interactions between Re and its NN atoms in the system.

Fig. 8 shows the electron density difference of the misfit interface system when Re is substituted for Ni in the γ phase and for Al in the γ' phase. From Fig. 8 we can also find that the bonding strength between Re and its NN host atoms is strongly increased after the substitution of Re for Ni or Al, especially the bonding between the atoms crossing the γ/γ' interface, which indicates how the addition of Re might influence the dislocation slipping along the γ/γ' interface. The above results are consistent with the analysis on interatomic energy presented in the previous section.

4. Summary

The doping effect of Re atoms on the γ phase, γ' phase and the γ/γ' interface of Ni-based single-crystal superalloys have been studied using MD simulation and the first-principles DVM. From MD relaxation it is found that on the γ/γ' interface there are only two atomic configurations, i.e. a coherent region and a misfit dislocation region; the "cage-like" misfit dislocation networks consist of $\langle 011\rangle\{100\}$ edge dislocations, winding over the precipitate phase. The MD simulations also show that Re would stabilize both the γ phase and the γ' phase, have a stronger Al site preferences in the γ' phase, induce localized lattice distortion, and influence the mismatch of the γ/γ' phase. The MD simulations demonstrate that Re atoms have a tendency to cluster in both the γ phase and the γ' phase, and the minimum size of an Re cluster is about 12.2 Å.

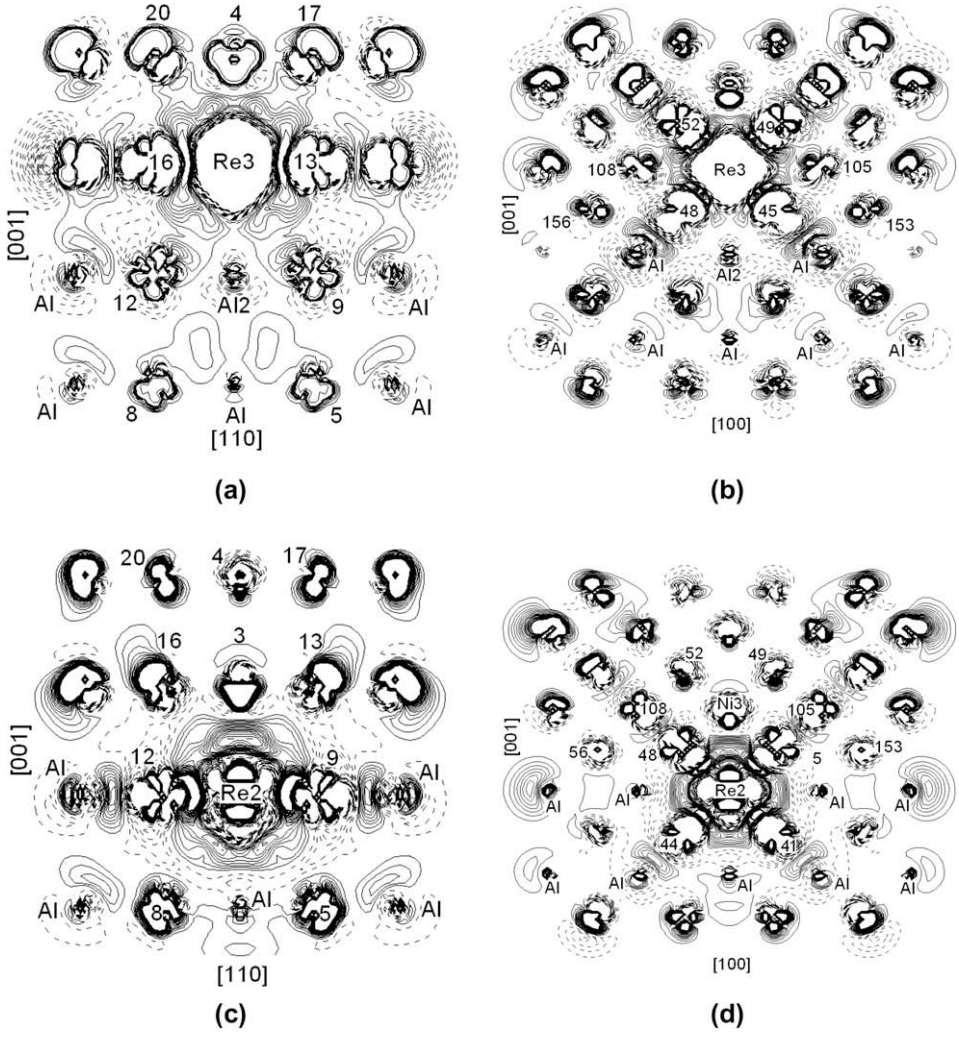

Fig. 7. The electron density difference of the coherent region of the Re-doped system. (a) and (b) are for the cases where Re is substituted for Ni in the γ phase; (c) and (d) are for the cases where Re is substituted for Al in the γ' phase. The Arabic numerals in Re3, Al2, etc., correspond to those in Fig. 4a. The unlabelled atoms are Ni atoms. The contour spacing is 0.0002e a.u.$^{-3}$. Solid lines and dashed lines correspond to the gain and the loss of electrons, respectively.

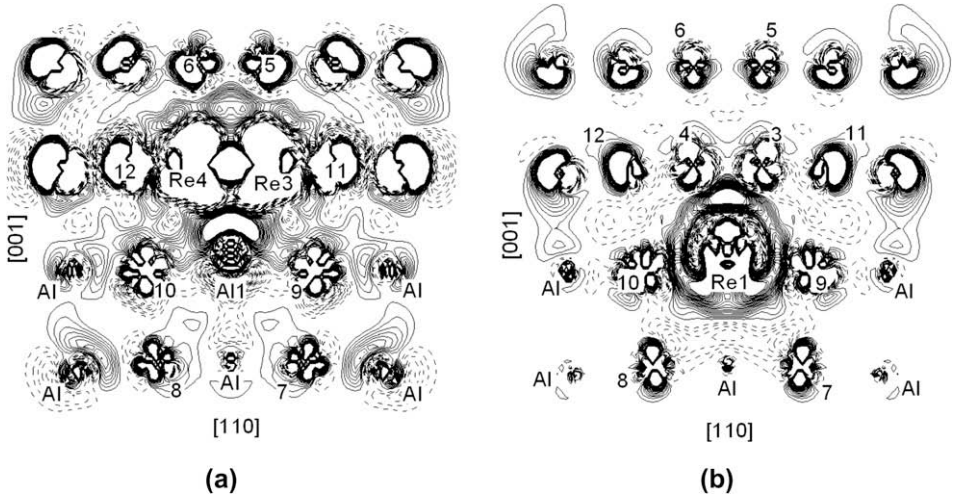

Fig. 8. The electron density difference of the misfit interface system of the Re-doped system. (a) is for the case where Re is substituted for Ni in the γ phase and (b) is for the case where Re is substituted for Al in the γ' phase. The Arabic numerals in Re3, Al2, etc., correspond to those in Fig. 4b. The unlabelled atoms are Ni atoms. The contour spacing is 0.0002e a.u.$^{-3}$. Solid lines and dashed lines correspond to the gain and the loss of electrons, respectively.

DVM calculation shows the first-principles results of the effect of Re on the electronic structure of the γ/γ' interface. It is found that a Re atom occupying either a Ni site in the γ phase or an Al site in the γ' phase can strongly enhance the bonding strength between Re and its NN atoms, indicating that the substitution atom Re will influence dislocation motion along the γ/γ' interface.

Acknowledgments

T.Z. would like to express his sincere thanks to Dr. Hongli Dang and Dr. Xiaolin Shu for their helpful discussions. This research was supported by the National Basic Research Program of China (Nos. 2000067102 and 2006CB605102), the National Natural Science Foundation of China (No. 90306016) and the China Postdoctoral Science Foundation (No. 20070420392).

References

[1] Jackson JJ, Donachie MJ, Henricks RJ, Gell M. Metall Trans A 1977;8:1615.
[2] Gell M, Duhl DN, Giamei AF. In: Tien JK, Wlodek ST, Morrow III H, Gell M, Maurer GE, editors. Superalloys 1980. Metals Park (OH): ASM; 1980. p. 205.
[3] Giamei AF, Anton DL. Metall Trans A 1985;16:1997.
[4] Mishima Y, Ochiai S, Suzuki T. Acta Metall 1985;33:1161.
[5] Blavette D, Caron P, Khan T. Mater Scr Metall 1986;20:1395.
[6] Blavette D, Caron P, Khan T. In: Reichman S, Duhl DN, Maurer G, Antolovich S, Lund C, editors. Superalloys 1988. The Metallurgical Society; 1988. p. 305.
[7] Lahrman DF, Field RD, Darolia R, Fraser HL. Acta Metall 1988;36:1309.
[8] Walston WS, O'Hara KS, Ross EW, Pollock TM, Murphy WH. In: Kissinger RD, Deye DJ, Anton DL, Cetel AD, Nathal MV, Pollock TM, et al., editors. Superalloys 1996. Warrendale (PA): TMS; 1996. p. 27.
[9] Erickson GL. In: Kissinger RD, Deye DJ, Anton DL, Cetel AD, Nathal MV, Pollock TM, et al., editors. Superalloys 1996. Warrendale (PA): TMS; 1996. p. 35.
[10] Murakami H, Saito Y, Harada H. In: Kissinger RD, Deye DJ, Anton DL, Cetel AD, Nathal MV, Pollock TM, et al., editors. Superalloys 1996. Warrendale (PA): TMS; 1996. p. 249.
[11] Daw MS, Baskes MI. Phys Rev Lett 1983;50:1285; Daw MS, Baskes MI. Phys Rev B 1984;29:6443.
[12] Johnson RA. Phys Rev B 1988;37:3924; Oh DJ, Johnson RA. J Mater Res 1988;3:471; Johnson RA, Oh DJ. J Mater Res 1989;4:1195.
[13] Johnson RA. Phys Rev B 1989;39:12554.
[14] Ellis DE, Painter GS. Phys Rev B 1970;2:2887.
[15] Baerends EJ, Ellis DE, Ros P. Chem Phys 1973;2:41.
[16] Averill FW, Ellis DE. Chem Phys 1973;59:6412.
[17] Ellis DE, Benesh GA, Byrom E. Phys Rev B 1977;16:3308.
[18] Delley B, Ellis DE. J Chem Phys 1982;76:1949.
[19] Delley B, Ellis DE, Freeman AJ, Baerends EJ, Post D. Phys Rev B 1983;27:2132.
[20] Hohenberg P, Kohn W. Phys Rev 1964;136:B864; Kohn W, Sham LJ. Phys Rev 1965;140:A1133.
[21] Zhang BW, Ouyang YF. Phys Rev B 1993;48:3022; Zhang BW, Ouyang YF, Liao SZ, Jin ZP. Physica B 1999;262:218.
[22] Hu WY, Zhang BW, Huang BY, Guo F, Bacon DJ. J Phys: Condens Matter 2001;13:1193.
[23] Zhang BW, Hu WY, Shu XL. Theory of embedded atom method and its application to materials science—atomic scale materials design theory. Changsha: Hunan University Publication Press; 2003.
[24] Kresse G, Hafner J. Phys Rev B 1993;47:558; Kresse G, Furthmuller J. Phys Rev B 1996;54:11169.
[25] Kresse G, Joubert D. Phys Rev B 1999;59:1758.
[26] Shu XL, Wang CY. Physica B 2004;344:413.
[27] Zhu T, Wang CY. Phys Rev B 2005;72:014111.
[28] Wang FH, Wang CY, Yang JL. J Phys: Condens Matter 1996;8:5527.
[29] Wang FH, Wang CY. J Phys: Condens Matter 1997;9:4499.
[30] Wang SY, Wang CY, Sun JH, Duan WH, Zhao DL. Phys Rev B 2001;65:035101.
[31] Von Barth U, Hedin L. J Phys C5 1972:1629.
[32] Xu JH, Oguchi T, Freeman AJ. Phys Rev B 1987;36:4186.
[33] Zhang X, Wang CY. Acta Metall 2009;57:224.
[34] Bürgel R, Grossmann J, Lüsebrink O, Mughrabi H, Pyczak F, Singer RF, et al. In: Green KA, Pollock TM, Harada H, Howson TE, Reed RC, Schirra JJ, et al., editors. Superalloys 2004. Warrendale (PA): TMS; 2004. p. 25.
[35] Wang CY, Dou CY, Zeng YP, Cao L, Liu FS. In: Proceedings of international workshop on the physics of materials (Shenyang), abstracts; 1989. p. B5-1.
[36] Wang CY. Defect Diffus Forum 1995;79:125.
[37] Mulliken RS. J Chem Phys 1955;23:1833.
[38] Briant CL. In: Westbrook JH, Fleischer RC, editors. Intermetallic compounds: 1 principles. New York: Wiley; 1994. p. 895.